Measuring water repellency of individual particles: the new “micro-Wilhelmy Plate Method” and its applicability to soil

J. Vogel[1]

H. M. Balshaw[1]

***S. H. Doerr**[2]

R. Bryant[1]

[1] **College of Engineering , Swansea University, Singleton Park, Swansea, SA2 8PP.**

[2]**Geography Department, Swansea University, Singleton Park, Swansea, SA2 8PP.**

***Corresponding author - E-mail address: s.doerr@swansea.ac.uk**

Highlights

- We introduce a new technique that allows measuring water repellency of individual particles
- Two variants of the method each provide relatively simple and quick wettability assessments
- It showed naturally wettable bulk soils contained water repellent particles and *vice versa*

Abstract

Water repellency (hydrophobicity) of granular materials such as soil is usually assessed on bulk samples or arrays of grains, with their wettability being influenced by the often-variable properties of individual particles. Numerous methods exist to assess the wetting behaviour of granular bulk materials, whereas methods for determining the wettability of individual grains are scarce. Here we introduce a new technique, based on the Wilhelmy plate method and termed “micro-Wilhelmy plate method” (mWPM) that allows quantification of the water repellency of an individual particle.

We developed two complementary variants of the methods, which involve the rupture of a water lamella after a particle has been brought into contact with water and then withdrawn from it. They were applied to individual wettable or water repellent spherical glass of diameter 120 and 270 µm) and polymer particles (270 µm), as well as those of both wettable and natural water repellent particles (of similar size i.e. 120 to 270 µm) from sandy soils of the UK and the Netherlands. Spherical glass and polymer particles were examined in their native condition and following contact with a hydrophobic (silicone-based water proofing) agent. In one method the break point of lamella was determined gravimetrically (g-mWPM, using an electronic 5-digit balance) and in the other it was determined optically (o-mWPM) from a video sequence obtained from a contact angle goniometer as the distance between the particle and the water surface at the point of lamella rupture. The latter required the use of image analysis and computation to estimate the potential energy of the water lamella.

Both methods provided meaningful assessments of particle wettability. Man-made particles showed limited variability, whereas those drawn from naturally wettable or water repellent soils exhibited substantial variability, indicating that wettable soils contain water repellent particles and *vice versa.* Both methods introduced here offer a relatively quick examination of the wettability of individual particles. The o-mWPM is a particularly simple method only requiring a video camera, stepper-motor driven sample holder and a low magnification optical system. Additionally, it offers the possibility to investigate particle shape.

Keywords

Soil water repellency; Wilhelmy Plate Method; soil particle; contact angle; hydrophobicity

1. Introduction

Water-repellency is a common feature of soils in many regions (Doerr et al., 2000; Mao et al., 2019) and a property of a wide range of man-made granular or powdery materials (Chawla et al., 1994). It is usually assessed on bulk samples or arrays of grains, with their wettability being influenced by the often-variable properties of individual particles (Doerr et al., 2000; Woche et al., 2005). Commonly used methods for investigating the wetting behaviour of powdered or granular materials are the capillary rise method (Preuss et al., 1998; Matthews et al., 2008) and a modified Wilhelmy Plate Method (WPM; Bachman et al., 2003; Woche et al., 2005). For the former, a theoretical liquid solid contact angle (CA) is calculated based on the height water is drawn into a tube filled with the powder, for the latter powder is fixed on a plate and then brought into contact with water. Details of the underpinning theory for these methods are given in Bachmann et al. (2003). Both methods provide data for powdered or granular material averaged over many particles rather than for individual particles. This is useful if the materials under investigation are chemically homogenous and have a very narrow size distribution. Polydisperse materials, such as soil, however, may exhibit a range of wettability within any particular sample, which will affect the overall wettability of the bulk material. The ability to estimate individual particle wettability is important in facilitating comparisons with data obtained from other (microscopic) particle investigations such as Scanning Electron Microscopy (Cengiz et al., 2004; Jiménez-Pinilla et al., 2016), or Atomic Force Microscopy (Cheng et al., 2009; Gazze et al., 2018). However, to date there is scarcity of methods allowing to determine the wettability of individual particles. Here we present a new method for estimating the wettability of individual particles.

The method exploits the principles of sphere tensiometry, which has been applied to the measurement of both interfacial tension in fluid systems and CA at solid liquid interfaces using the same principles as the WPM (Scheludko et al., 1975; Huh et al., 1976). WPM measures the force required to detach a solid sample from a liquid surface, which is proportional to the surface tension of the liquid. The technique is mostly used to determine

the surface tension of liquids, but can also be used to determine CAs between a solid and a liquid of which surface tension is known (e.g. Chawla, 1994; Gilboa et al., 2006; Richter et al., 2006). The CA is calculated directly from the force measurement (providing that the geometry of the sample is known) or is measured directly as the angle formed between the solid and the tangent to the liquid lamella at the point of contact. This method has, for example, been used in a modified form to provide an assessment of the wettability of bulk soils, whereby soil particles are attached to glass slides. Measurements of advancing and receding contact angles are determined with the use of a precision tensiometer (Bachman et al., 2003). In contrast to the WPM, which measures the detachment force between liquid and solid, sphere tensiometry records force as a spherical sample is drawn through the interface between the two phases. Using clean materials and precise instrumentation the latter is a sophisticated method for determining the liquid-solid CA at a surface (Fieber et al., 1979).

As the development of our new method is based on the principles of WPM, it is introduced here as the “micro Wilhelmy plate method” (mWPM). Two different approaches were used to obtain data: (i) optical measurements (“o-mWPM”) and (ii) gravimetric measurements (“g-mWPM”). These approaches were both applied to homogenous spherical particles of contrasting wettability (model particles). The o-mWPM was further applied to individual particles drawn from a selection of sandy soil samples, with contrasting bulk soil wettability in order to (a) test the applicability of the method to soil particles and (b) explore the distribution of individual particle wettability within the natural soils the particles were drawn from.

2. Materials and Methods

Hydrophilic small and large glass ballotini (beads) with average diameters of 120 μm and 270 μm (denoted here as GS and GL respectively) were divided and subsamples thoroughly mixed with FabsilTM (a silicon based water repellent liquid formulation designed for the treatment of textiles, Grangers UK), and left to dry, rendering them strongly water repellent

(GS_{wr} and GL_{wr} resp.). To test the persistence of this water repellent treatment, particles were sprinkled onto a water surface of sufficient depth to prevent evaporation from depleting the water body. The proportion of particles remaining on the water surface after 1 min and 48 h after addition was found to be the same, demonstrating sufficient persistence of the induced water repellency for the purpose of this study. Wettable to slightly hydrophobic polymethylmethacrylate ballotini (PMMA, Diakon®) with an average diameter of 270 µm (DIA) were obtained from Distrupol UK. In addition to these model particles, natural particles from sandy soils in the Netherlands and the UK were sampled from water repellent (NLwr and UKwr and directly adjacent wettable (control) soil (NLc and UKc) respectively (Table 1). Their size distribution was determined using a laser diffraction particle size analyser (Malvern Mastersizer, UK) and their potential persistence of water repellency determined on dry bulk samples using the Water Drop Penetration Time method (WDPT; Bisdom et al., 1993). We also conducted CA measurements on bulk particle layers (Table 1) as described below. More details about the soils used can be found in a study examining natural organic compounds therein causing water repellency (Doerr et al., 2005), in which soils NLwr and UKwr were denoted NL2 and UK1 respectively.

2.1 Contact Angle (CA) measurements on soil particle layers

Specimens were prepared by sprinkling the soil particles on to a glass microscope slide whose surface was covered with double-sided adhesive tape. The slide was then tapped gently against the bench top to remove loose material. CAs of these specimens were measured using a goniometer (Easydrop DSA100, Kruess GmbH, Hamburg, Germany; software DSA Version 1.900.14). A droplet of water (~15 µl) was placed on the sample surface, using a software controlled stepper-motor-driven syringe and images of it were recorded by camera at 1.67 frames per second for a total of 60 s. The contact angle was

135 then calculated using the software. The average contact angle determined from 10 images
136 obtained at 5 s intervals during the period 7 – 60 s is reported here (Bachmann et al., 2000).

137

138 *2.2. Particle wettability determination using the optical micro Wilhelmy plate*
139 *method (o-mWPM)*

140 Individual particles were selected randomly from the bulk sample material and each was
141 placed on a glass slide using the tip of a needle. Each was then affixed to the middle of a
142 microscope cover slip using waterproof cyanoacrylate adhesive (Anglin' glue®, Fisherman's
143 choice, UK). A total of ≥15 particles per sample were selected. Each cover slip (bearing an
144 individual particle) was then fixed to a device, consisting of a stainless-steel tube enveloping
145 a longer steel rod that was fitted with disks on both ends, designed to fit the syringe holder of
146 the goniometer described above. The upper disk was clamped into the syringe holder of the
147 goniometer where its vertical position and speed of adjustment were controlled using the
148 instrument's stepper motor (via the associated computer). The particle was thus suspended
149 from the lower face of the horizontal cover slip. A glass cover slip was attached to the lower
150 platform, using double sided adhesive tape, upon which a clean glass microscope slide was
151 placed. A distilled water drop (~1 ml) of sufficient volume to create a planar water surface
152 was placed on this slide underneath the particle. The particle was then lowered towards the
153 water at a speed of 0.011 mm s^{-1} (Fig. 1a). When it contacted the water surface it was
154 stopped and retracted (Fig. 1b) until the attached water lamella broke. These events were
155 recorded using the instrument's video camera at a frame rate of 30 Hz.

156 A video frame showing the water surface with the particle remote from it was used to
157 determine the reference height of that surface and provided a baseline; the frame
158 immediately prior to the rupture of the lamella on retraction of the particle was also selected.
159 (Fig. 2). The images were then evaluated using SigmaScan Pro 5® software (SYSTAT
160 Software Inc.). Data markers were placed to identify the diameter of the particle, the detail of

161 the curvature of the water drop, the wetted perimeter and at the midpoint of the particle.
162 Additional data markers were set at cross points of a horizontal line through the lowest point
163 of the particle and the water line. The intersection of baseline and water lamella was
164 calculated from these data.

165 The data, as frame pixel co-ordinates, were exported and converted to metric units using the
166 image magnification which was held constant throughout (0.514/278 mm pixel^{-1}).

167 Assuming the particle to be spherical, we then calculated: i) the distance (h) between the
168 free liquid surface (baseline) and the base of the particle, ii) the particle diameter (d), iii) the
169 wetted diameter of the particle (d_w), iv) the volume (V) of water drawn between the free
170 surface and the particle (assuming circular symmetry), v) the increase in potential energy of
171 that water (E_{pot}), relative to the free surface and, vi) the wetted perimeter L (the contact line
172 of liquid on the solid), from the wetted diameter (assuming a spherical particle shape).

173 The volume of water and the potential energy were calculated by numerical integration and
174 rotation about the axis. It was possible to consider the volume as a stack of cylinders or set
175 of cylindrical annuli, which are rotated around the y axis, allowing both approaches to be
176 used and their outcomes to be compared. As the chosen elements could lie on either side of
177 the particle and, in some cases, lateral asymmetry occurred, integrations were performed
178 independently using data associated with the individual sides. In doing so, several estimates
179 of V and E_{pot} were available for comparison. Two numerical integration procedures were
180 carried out: (i) a cubic spline integration, using cubic polynomials for piecewise integration
181 over subintervals (Schwarz et al., 1986) and (ii) trapezium integration employing the rule
182 where an element under the curve is approximated to a trapezium (Merziger et al., 1996).
183 Four integrations were carried out for each side of each particle comprising cubic spline and
184 trapezium integrations with rotation around the y-axis.

185

2.2. Particle wettability determination using the gravimetric micro Wilhelmy plate method (g-mWPM)

An individual particle was randomly chosen and glued to the narrow edge of a microscopic glass slide using double sided adhesive tape. The microscopic slide was then inserted into the holder of a tensiometer (DCAT 21, DataPhysics Instruments GmbH, Filderstadt, Germany), which was connected to an electronic 5-figure precision balance and a PC running SCAT11 software (DataPhysics Instruments GmbH) to control the tensiometer.

With the specimen in place, the balance was set to zero and the sample was slowly lowered, at a speed of 0.01 mm s^{-1}, into a container of water at 20 °C. The weight change necessary to trigger a measurement was set to 0.08 mg and immersion depth of the sample was set to 0.06 mm and 0.1 mm. This was measured from the point at which the balance registered the required weight change. After some initial trials involving the use of both depths it was found that the precision and value of the lamella breakpoint was similar in both cases (Table 2), so the immersion depth of 0.1 mm was selected for further work.

The software recorded the weight of the water pulling on the sample in relation to the position of the sample (*ps*) with the point of origin set at the maximum immersion depth. As the specimen was withdrawn, a water lamella was pulled up and the weight registered on the balance increased. Close to the breakpoint of the lamella, the weight of the water lifted by the particle reached a maximum and the CA between water lamella and particle was reduced to zero. The lamella then thinned as water drained from it under the influence of gravity. This process happened quickly (in the range of ms) and within a short distance (~0.05 mm) of the water lamella breakpoint. A tangent was drawn on the curve of weight as a function of position (Fig. 3) between points B and C and a horizontal line drawn at maximum weight. The intersection between these was defined as the lamella breakpoint.

This point may not represent the real height of the water lamella pulled up by the particle as the height measurement only starts at the moment of the defined weight change. The

lamella break point, therefore, is not referred to as lamella height, but as ps (Equation 1). All values were also corrected by the immersion depth of 0.1 mm and the starting value C_S ~ 0.4 mm for all samples, so that:

$$ps = B - 0.1\ mm - C_s \quad \text{(Equation 1)}$$

3. Results

3.1. o-mWPM method

The lamella height of water pulled up by an individual particle was considered to provide a measure of the wettability of that particle. A linear correlation (with r ~ 1) between lamella height (*h*) and CA (θ) of the bulk material on a flat surface was found for the materials GL, DIA and GLwr (Fig. 4a). Mean values of *h* for 120 µm ballotini (GS) and 120 µm hydrophobized glass ballotini (GSwr) were about 0.05 mm smaller than those of 270 µm ballotini (GL) and 270 µm hydrophobized glass ballotini (GLwr), respectively. Glass beads GL and GLwr, as well as Diakon ballotini (DIA), had a similar mean diameter, whereas the glass beads GS and GSwr were about half that size. The differences between *h* of the samples GL, GLwr and DIA were significant (p = 0.01). The influence of particle size was reduced by utilization of the dimensionless ratio *h/d* with *d* being the individual particle diameter (Fig. 4b). This reduced the difference between the mean *h* of wettable glass ballotini GS and GL, and had a similar effect on water repellent glass ballotini GLwr and Gwr. The wettable GS and GL group was found to be significantly different from the water repellent GLwr and GSwr group (p = 0.01). *h/d* reduced the difference between GL, GS and DIA samples. Both GL and GS materials were wettable and can be clearly differentiated from water repellent glass beads (GLwr and GSwr).

236 Box plots indicating the nature of the distribution of h/d for the various particles show GL to
237 have the broadest distribution with a minimum value extending beyond the bulk of the data
238 for GSwr and GLwr (with the bulk of their values below GS and the other non-wr particles).
239 The central 80% of the distributions of GL and GLwr are of similar width with the latter
240 showing significantly different values of h/d, corresponding to the difference in the surface
241 chemistry between their wettable and water repellent surfaces respectively.
242

243 ## *3.2. g-mWPM method*

244 Water lamella attached to large particles (GL, DIA and GLwr), subject to the gravimetric
245 mWPM method, ruptured at various different heights (*ps*) relative to the free liquid surface
246 with GLwr being the lowest and with the highest CA (Fig. 6a). GL and DIA had similar p
247 values but significantly different CAs. Ratios of *ps* to the wetted particle perimeter (*L*)
248 estimated from the maximum force (F_{max}) (Equation 2), the mass of water (*m*) and its surface
249 tension (y_L) provide an improved correlation with CA (Fig. 6b).

250

251 $$F_{max} = m\ g = L\ y_L \cos\theta \qquad \text{(Equation 2)}$$

252 The CA θ was assumed to be zero at maximum force (see Fig. 3b); thus, *L* (Equation 3) was
253 calculated as:

254 $$L = \frac{m\ g}{y_L} \quad \text{(Equation 3)}$$

255
256

257 ## *3.3. Results of application of the o-mWPM to soil particles*

258 The distributions of lamella height obtained from the analysis of individual particles selected
259 from wettable and water repellent soils showed significant overlap (Fig. 6). Data from o-
260 mWPM showed that the range of *h* for the wettable soil UKc falls within that of the water
261 repellent soil UKwr, but the latter shows a majority of values below that of UKc (Fig. 7a). The

width of the distribution of data for UKwr is larger than that of UKc. In contrast, distributions for both wettable soil NLc and water repellent soil NLwr were similar.

The UK soil particles had significantly larger normalised height distributions (*h/d)* from those of the NL soils (Fig. 7b). The *h/d* distribution for UKc was found to fall well within that of UKwr and, as for *h*, no difference between NLwr and NLc was found. The distribution width of *h/d* for UKwr was again larger than that for UKc. Lamella height *h* normalised by the wetted perimeter *L* also showed that the UKc distribution falls well within the limits of UKwr and the two are essentially indistinguishable from each other. The distributions of the NL pair are also similar, but with means, medians and limits above those of the UK samples. Both water repellent samples show a broader *h/L* distribution than the wettable ones (Fig. 7c). The mean lamella heights of UKwr and UKc samples were higher than those of any model particle material used, whereas NLwr and NLc both have a mean *h* similar to that of DIA. Mean *h/d* values of both UK samples are between those of GL and GLwr. Both NL samples have mean values in the region of that of SGwr (Fig. 5).

3.4 Reproducibility of measurements

Repeated immersion and retraction of particles in a plane water surface (without providing sufficient time for the particle surface to dry) resulted in lamella of random heights (with a relative standard deviation of ~6%) without any indication of a trend to higher or lower values. Similar repeated measurements of both ballotini and soil particles following rotation in the image field by 90° indicated that ballotini diameters were consistent with the symmetrical shape whereas those for soil particles varied considerably with the direction of observation. The asymmetry of these particles therefore introduces another source of variance which requires consideration in relation to estimates of E_{pot} and E_{pot}/d.

4. Discussion

4.1 Comparison of o-mWPM and g-mWPM

Both methods for examining the interaction of a particle with a free water surfaces (o-mWPM and g-mWPM) involve bringing it into contact with that surface and then raising it to form a water capillary or lamella which eventually ruptures. Absolute values of *h* calculated from images obtained by o-mWPM and *ps* recorded by g-mWPM for particles of similar size and properties were found to differ. Nevertheless, and despite the few degrees of freedom, a linear correlation was found between the two methods (r =0.97, Fig. 8). The data deviate from the 1:1 line, indicating a systematic difference between the methods that is probably due to the different principles underlying the measurements (and which may be amenable to calibration). The determination of *ps* from the g-mWPM is an approximation of the lamella height. This in turn is dependent on the precision and accuracy of the balance in relation to detecting the weight change that triggers measurements. The o-mWPM introduces an uncertainty in the measurement of the lamella height due to the frame rate of the camera. Use of a higher speed camera would allow observation of the thinning of lamella and precise location of its breakpoint, provided that adequate resolution of the images is maintained so as to avoid transfer of the uncertainty to linear measurements. In the present work the standard error of the mean *h* and *ps* of all samples is similar for o-mWPM and g-mWPM, suggesting a comparable level of precision for both methods. Compensation for variation in particle size by considering *h/d* or *ps/L* appears to be useful as it reduces the differences associated with material of the same surface properties (such as glass ballotini). The similarity in the quality of correlations involving E_{pot}/d and *h/d* suggest that the latter might just as well be used for comparison with other data as it is readily amenable to direct evaluation from the appropriate video frames. The more detailed, and more time consuming, evaluation of E_{pot} seems unwarranted as it presently involves a higher degree of subjectivity in defining the lamella surface.

Both o-mWPM and g-mWPM are able to detect differences between individual model particles of different wettability. The o-mWPM facilitates estimates of particle diameter and wetted perimeter, but evaluation of data obtained by g-mWPM requires fewer resources than o-mWPM although any facility for estimating particle dimensions will require additional resources.

4.2. mWPM applicability to soil and implications for soil water repellency

The wide range of lamella heights (*h*) obtained from particles drawn from the same soil sample strongly suggests that wettability is a variably distributed property. This in turn supports the suggestion made in previous studies examining organic coatings on particles drawn from water repellent soils using Atomic Force Microscopy that expression of water repellency in a sample need not arise from particles with uniform surface distribution of water repellent properties (Cheng et al., 2009; Gazze et al., 2018). These properties are likely to be distributed both around individual particles and between them within a sample. This also agrees with work suggesting that behaviour of the bulk material may be influenced by the presence of a small proportion of hydrophobic particles (Bisdom et al., 1993; Bauters et al., 1998; Bachmann et al., 2000). The present study suggests that *h* or *h/d* may serve as parameters of particle wettability where, at least, the net effect of all the different types of surface available on the wetted particle surface are reflected in the measurement.

The wide distributions of *h/d* and *h/L* for particles drawn from UKwr and NLwr soils suggest that there is a considerable range of individual particle wettability associated with soils exhibiting water repellency in comparison with those that are readily wettable. Nearly all particles within wettable soil samples can be considered to be wettable. Only a small proportion of water repellent particles appear to be necessary for a soil to exhibit water

repellency (where many particles are involved in the assessment, Bisdom et al., 1993; Bauters et al., 1998; Bachmann et al., 2000).

Application o-mWPM and g-mWPM to approximately isometric particles drawn from sandy soils show that h/d or h/L are useful in compensating for the effect of particle size. The orientation of particles of more irregular shape may need to be considered and a more appropriate estimate of an equivalent circular diameter or wetted perimeter obtained from a more detailed examination of the particle as it is rotated about the axis normal to the water surface. Previous work on soil aggregates suggested the use of an equivalent diameter, such as use of a mean circular diameter of an aggregate (Dexter et al., 1985) which is readily obtained for individual particles using the facilities of the o-mWPM method described here. Given that the method has been tested here on particles down to 120 μm in size, in future work it would be useful to explore the lower limit of particle size to which it can be applied.

The data obtained here also suggest that particles from the water repellent sample NLwr may have a rather broad range of wettabilities, given that the variation in reduction is highest for this sample. Previous studies of the same soils have shown that NLwr and UKwr contain high proportions of large polar compounds (Doerr et al., 2005; Mainwaring et al., 2004). If the distribution of water repellency is much broader in NLwr than in UKwr this may indicate a possibly more irregular distribution of such compounds on the particles in NLwr than in UKwr. The difference between UKc and NLc, although both are completely wettable and contain only very small amounts of total organic material (Table 1), may indicate that other influences apart from the surface chemistry may be of importance. These could be roughness and particle size, the latter of which may not be completely compensated by *d* or *L* as characteristic linear dimensions of the particles by which to scale lamella height.

The more widely scattered *h* values obtained from particles of UKc in comparison with the narrower ranges of *h/d* and *h/L*, seem to reflect the relatively broad particle size range of this

soil sample, whereas the similarity of the particle size distributions of NLwr and NLc suggests that size is an insignificant property affecting the variation in particle or bulk soil wettability of these samples.

The general difference between the two sample pairs NL and UK may arise from particle mineralogy, surface roughness and chemistry. In order to use the m-WPM to determine absolute particle wettability, a thorough calibration using standard materials of various known wettabilities is required. This should ideally involve particles of similar roughness and shape to the particles under test.

The almost consistent reduction in lamella height following addition of the hydrophobic agent to individual particles suggests that this simple method of application provides some degree of consistency.

The mWPM offers a relatively quick examination of individual particle wettability drawn from particulate materials. The o-mWPM is a simple method only requiring a video camera, stepper-motor driven sample holder and a low magnification optical system. Additionally, it offers the possibility to investigate particle shape. Data analysis is presently time-consuming requiring a minimum of two images per particle per analysis and ~15 minutes for image evaluation and calculation. Data evaluation of the g-mWPM is faster and mostly automated and, consequently, less dependent on subjective judgements made by the operator (in the o-mWPM) for use in subsequent data processing. The addition of an optical component could facilitate evaluation of particle shape.

If both methods are applied in combination to soil or other particles, whereby images of the particle and water lamella are obtained together with the force measurement by tensiometry this could provide more detailed information about rate of draining of water from the lamella and its rupture. In combination with information about particle size and shape, this could provide useful insights on the nature of the chemical characteristics of the outermost surface of the particles, which together with the shape and topography of the particle surface,

determines overall particle wettability (Zisman, 1964; McHale et al., 2005; Gazze et al., 2018). Using a substantially higher frame rate than used here may improve precision of the moment of lamella rupture and provide detail of lamella thinning as this moment is approached.

5. Conclusions

Both micro-scale adaptations of the Wilhelmy plate method (WPM) were shown to be effective in detecting differences between both the wettability of model spherical particles of various types and of particles of the same type before and after treatment to render them hydrophobic. This suggests that this new method can be applied effectively as a comparatively simple, non-destructive approach for detecting relative differences in the wettability (water repellency) between particles. o-mWPM facilitates estimates of particle diameter and wetted perimeter, but evaluation of data obtained by g-mWPM requires fewer resources than o-mWPM.

Individual particles drawn from sandy soils with known bulk wettability (WDPT) produced a wide range of wettabilities, with at least 15 individual particle measurements being insufficient to quantitatively predict bulk soil wettability. This suggests that particle wettability in these samples was heterogenous, which in turn supports the notion that water repellency in soils, at this scale, is a distributed property. Notwithstanding this, the position and width of the distributions providing these statistics qualitatively reflect the difference between the wettability of the bulk soil in terms of the groups: *h/d* and *h/L*. However, where the geometry of the particle is known and reference material with known (and reproducible) wettability is available then a more quantitative approach may be possible as could be the case for manufactured granular material.

6. References

Bachmann, J., Ellies, A. and Hartge, K.H. (2000) Development and application of a new sessile drop contact angle method to assess soil water repellency. *Journal of Hydrology,* 231-232, 66-75.

Bachmann J., Woche, S. K., Goebel, M.-O., Kirkham, M. B. and Horton, R. (2003) Extended methodology for determining wetting properties of porous media. *Water Resources Research,* 39 (12), 1353.

Bauters, T., DiCarlo, D., Steenhuis, T. and Parlange, J.-Y. (1998) Preferential flow in water-repellent sands. *Soil Science Society of America Journal,* 62, 1185-1190.

Bisdom E.B.A., Dekker L.W. and Schoute J.F.T. (1993) Water repellency of sieve fractions from sandy soils and relationships with organic material and soil structure. *Geoderma,* 56, 105-118.

Cengiz, S., Karaca, A.C., Çakır, I., Üner, H.B. and Sevindik, A. (2004) SEM–EDS analysis and discrimination of forensic soil. *Forensic Science International,* 141, 33-37

Chawla, A.B., Buckton, G., Taylor, K.M.G., Newton, J.M. and Johnson, M.C.R. (1994) Wilhelmy plate contact angle data on powder compacts: considerations of plate perimeter. *European Journal of Pharmaceutical Sciences,* 2, 29-39.

Cheng, S., Bryant, R., Doerr, S.H., Wright, C.J. and Williams R. (2009) Investigation of physico-chemical surface properties of soil particles and model materials with contrasting hydrophobicity using atomic force microscopy. *Environmental Science and Technology*, 43, 6500–6506.

de Gennes, P.G., Brochard-Wyart F. and Quéré D. (2004). Capillarity and wetting phenomena: drops, bubbles, pearls, waves. New York. Springer Science & Business Media Inc.

438 Doerr, S.H., Shakesby, R.A. and Walsh, R.P.D. (2000) Soil water repellency: its causes,
439 characteristics and hydro-geomorphological significance. *Earth Science Reviews,* 51, 33–65.

440 Doerr, S.H., Llewellyn, C.T., Douglas, P., Morley, C.P., Mainwaring, K.A., Haskins, C.,
441 Johnsey, L., Ritsema, C.J., Stagnitti, F., Allinson, G., Ferreira, A.J.D., Keizer, J.J., Ziogas,
442 A.K. and Diamantis, J. (2005) Extraction of compounds associated with water repellency in
443 sandy soils of different origin. *Australian Journal of Soil Research*, 43(3), 225-237.

444 Dexter, A.R. and Kroesbergen B. (1985) Methodology for determination of tensile strength of
445 soil aggregates. *Journal of Agricultural Engineering Research / publ. for the British Society*
446 *for Research in Agricultural Engineering,* 31, 139-147.

447 Fieber, C. and Sonntag, H. (1979) Theoretical consideration on the applicability of the
448 sphere method for measuring interfacial-tension and contact-angle. *Colloid and Polymer*
449 *Science,* 257, 874-881.

450 Gazze, S.A., Hallin, I., Quinn, G., Dudley, E., Matthews, P.G., Rees, P., Van Keulen, G.,
451 Doerr, S.H. and Francis, L.W. (2018). Organic matter identifies the nano-mechanical
452 properties of native soil aggregates. *Nanoscale*, 10(2), 520-525.

453 Gilboa A., Bachmann J., Woche S.K. and Chen Y. (2006) Applicability of interfacial theories
454 of surface tension to water-repellent soils. *Soil Science Society of America Journal,* 70,
455 1417-1429.

456 Huh, C. and Mason, S.G. (1976) Sphere Tensiometry - evaluation and critique. *Canadian*
457 *Journal of Chemistry-Revue Canadienne De Chimie,* 54, 969-978.

458 Jiménez-Pinilla, P., Mataix-Solera, J., Arcenegui, J., Delgado, R., Martín-García, J.M.,
459 Lozano, E., Zavala, L.M., and Jordán, A. (2016) Advances in the knowledge of how heating
460 can affect aggregate stability in Mediterranean soils: a XDR and SEM-EDX approach.
461 *Catena*, 147, 315-324.

462 Mao, J., Nierop, K.G.J., Dekker, S.C.; Dekker, L.W., and Chen, B. (2019) Understanding the
463 mechanisms of soil water repellency from nanoscale to ecosystem scale: a review. *Journal*
464 *of Soils and Sediments*, 19, 171-185.

465 Mainwaring K.A., Morley C.P., Doerr S.H., Douglas P., Llewellyn C.T., Llewellyn G.,
466 Matthews I. and Stein B.K. (2004) Role of heavy polar organic compounds for water
467 repellency of sandy soils. *Environmental Chemistry Letters,* 2, 35-39.

468 Matthews, G.P., Watts, C.W., Powlson, D.S., Price, J.C. and Whalley, W.R. (2008). Wetting
469 of agricultural soil measured by a simplied capillary rise technique. *European Journal of Soil*
470 *Science* 59 (4), 817-823.

471 McHale, G., Newton, M. I. and Shirtcliffe, N. J. (2005). Water-repellent soil and its
472 relationship to granularity, surface roughness and hydrophobicity: a materials science view.
473 *European Journal of Soil Science*, 56, 445-452.

474 Merziger, G., Mühlbach, G., Wille, D. and Wirth, T. (1996). Formeln & Hilfen zur höheren
475 Mathematik. Hannover, Binomi.

476 Preuss, M. and Butt, H.-J. (1998) Measuring the contact angle of individual colloidal
477 particles. *Journal of Colloid and Interface Science*, 208, 468–477.

478 Richter, L. and Vollhardt, D. (2006) Force measuring methods for determination of surface
479 tension of liquids: a comparison. *Physical Chemistry,* 43, 256-261.

480 Scheludko, A.D. and Nikolov, A.D. (1975) Measurement of surface-tension by pulling a
481 sphere from a liquid. *Colloid and Polymer Science,* 253, 396-403.

482 Schwarz, H.R. and Köckler, N. (1986). Numerische Mathematik. Wiesbaden, B.G. Teubner
483 Verlag/GWV Fachverlage GmbH.

484 Woche, S.K., Goebel, M.O., Kirkham, M.B., Horton, R., Van der Ploeg, R.R. and Bachmann,
485 J. (2005) Contact angle of soils as affected by depth, texture, and land management.
486 *European Journal of Soil Science,* 56, 239-251.

487 Zisman, W. A. (1964) Relation of equilibrium contact angle to liquid and solid construction,
488 in *Contact Angle, Wettability and Adhesion*, edited by R. F. Gould, Advances in Chemistry
489 Series, 43, 1– 51.

490

491 **Table 1. Sample codes, origins, mean particle diameter and distribution width, Contact Angle**
492 **(CA) of multi-particle layer and Water Drop Penetration Times (WDPTs). UK = United Kingdom,**
493 **NL = The Netherlands; wr denotes 'water repellent' and c denote wettable 'control' bulk soil**
494 **behaviour.**

Code	Site Location/ origin	Latitude/ Longitude	Vegetation type	Sampled depth (cm)	Total organic carbon (mass %)	Mean diameter & distribution width (mm)	WDPT (s)
NLwr	Ouddorp	51°48'N, 3°54'E	Grass, moss	10-20	5.9	0.23; 0.10	4800
NLc	Ouddorp	51°48'N, 3°54'E	Grass, moss	30-40	<0.8	0.22; 0.07	<5
UKwr	Gower Peninsula	51°35'N, 4°06'W	Dune herbs, grasses	0-5	11.4	0.33; 0.08	>18000
UKc	Gower Peninsula	51°35'N, 4°06'W	Un-vegetated	0-5	3.1	0.39; 0.12	0
GS	Glass ballotini					120	
GSwr	Glass ballotini treated with FabsilTM					120	
GL	Glass ballotini					270	
GLwr	Glass ballotini treated with FabsilTM					270	
DIA	Polymethylmethacrylate ballotini (PMMA, Diakon®)					270	

495

Table 2: Position of sample (ps) at which lamella break occurred, calculated from different immersion depths for the following materials: 270 µm glass ballotini (GL), 270 µm Diakon (DIA) and hydrophobized glass ballotini (GLwr) for five particles per material using three repetitions for each immersion depth.

		ps [mm] for immersion depth	
		0.06 mm	**0.1 mm**
GL	1	0.52 ± 0.01	0.51 ± 0.01
	2	0.55 ± 0.01	0.53 ± 0.01
	3	0.45 ± 0.01	0.42 ± 0.01
	4	0.55 ± 0.01	0.54 ± 0.01
	5	0.47 ± 0.01	0.42 ± 0.01
DIA	1	0.44 ± 0.01	0.39 ± 0.01
	2	0.44 ± 0.07	0.46 ± 0.02
	3	0.39 ± 0.01	0.42 ± 0.01
	4	0.45 ± 0.01	0.42 ± 0.03
	5	0.47 ± 0.01	0.41 ± 0.05
GLwr	1	0.28 ± 0.01	0.25 ± 0.01
	2	0.31 ± 0.01	0.28 ± 0.02
	3	0.39 ± 0.02	0.37 ± 0.01
	4	0.27 ± 0.01	0.21 ± 0.02
	5	0.25 ± 0.01	0.25 ± 0.04

Table 3: Absolute and relative mean reductions of *h* after coating with Fabsil™

	***h* reduction in mm**	***h* reduction in %**
GL	0.16 ± 0.01	52.6 ± 1.4
DIA	0.15 ± 0.01	52.6 ± 1.8
NLwr	0.24 ± 0.04	38.7 ± 2.8
NLc	0.22 ± 0.01	45.6 ± 1.0

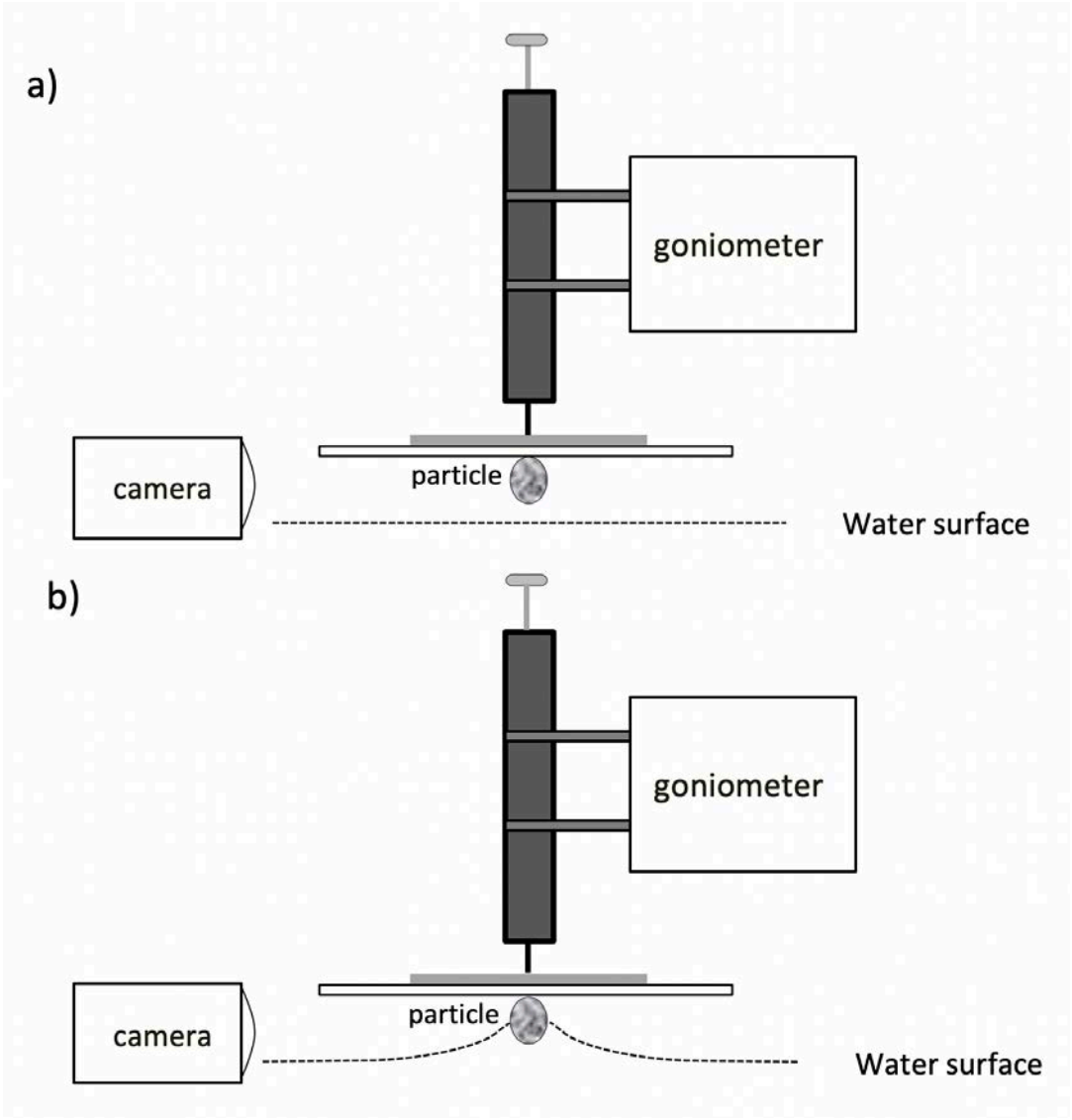

Figure 1. Diagram of a) approach of particle to water surface and, b) retraction of particle with water lamella attached.

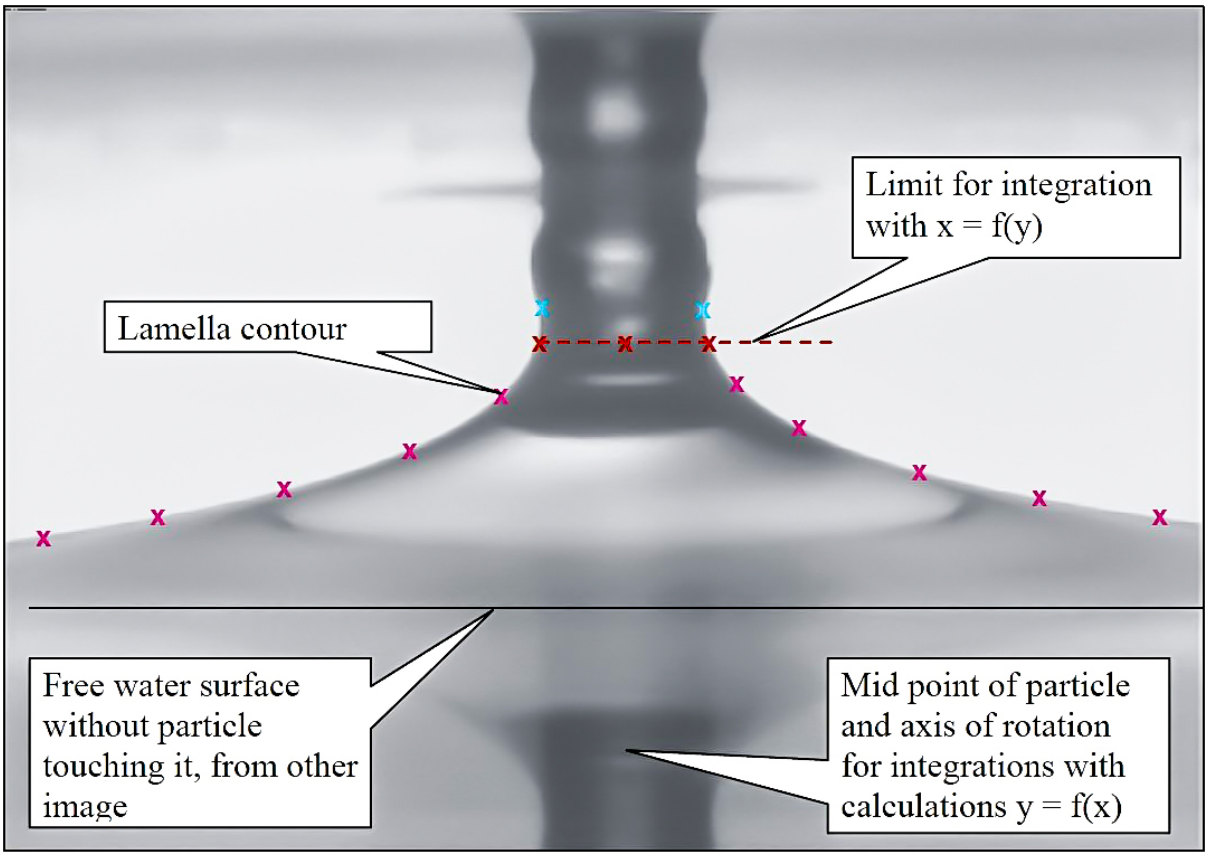

Figure 2. Determination of co-ordinates of the liquid surface just before the lamella breaks.

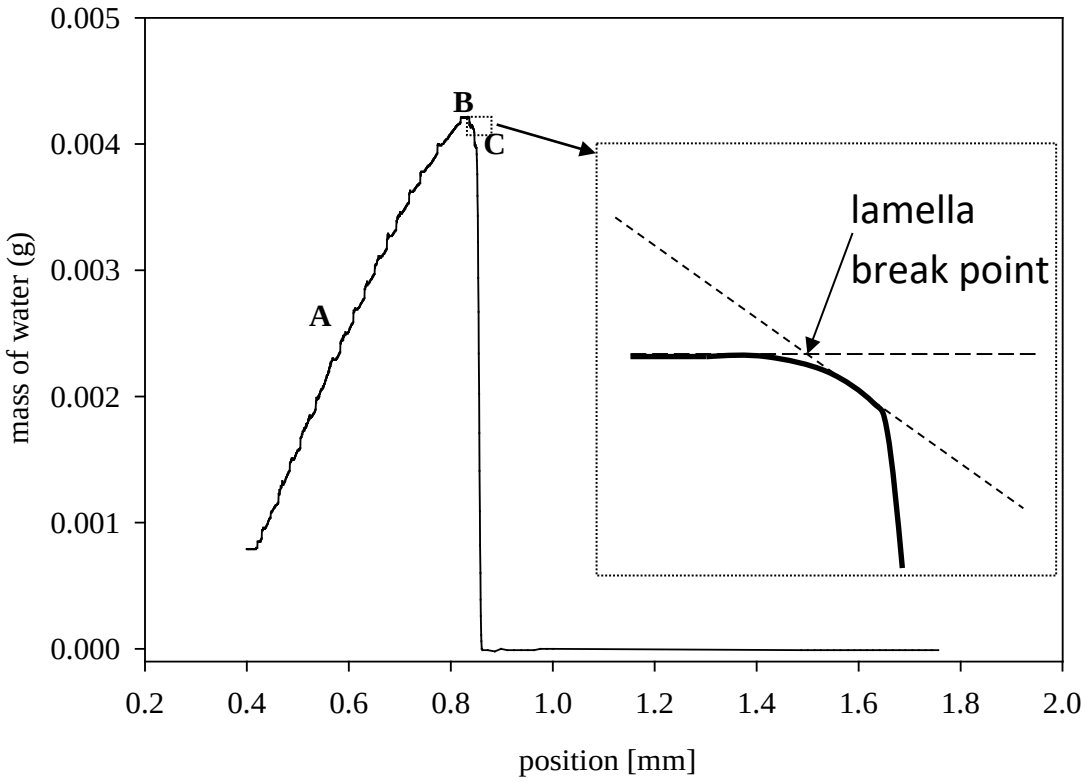

525

526 **Figure 3: Typical weight *vs* distance curve for a spherical particle: A) at increasing distance**

527 **from liquid surface, B) at maximum force/ maximum weight of water pulled up by sample, and**

528 **C) thinning liquid lamella reduces the force pulling on the particle.**

529

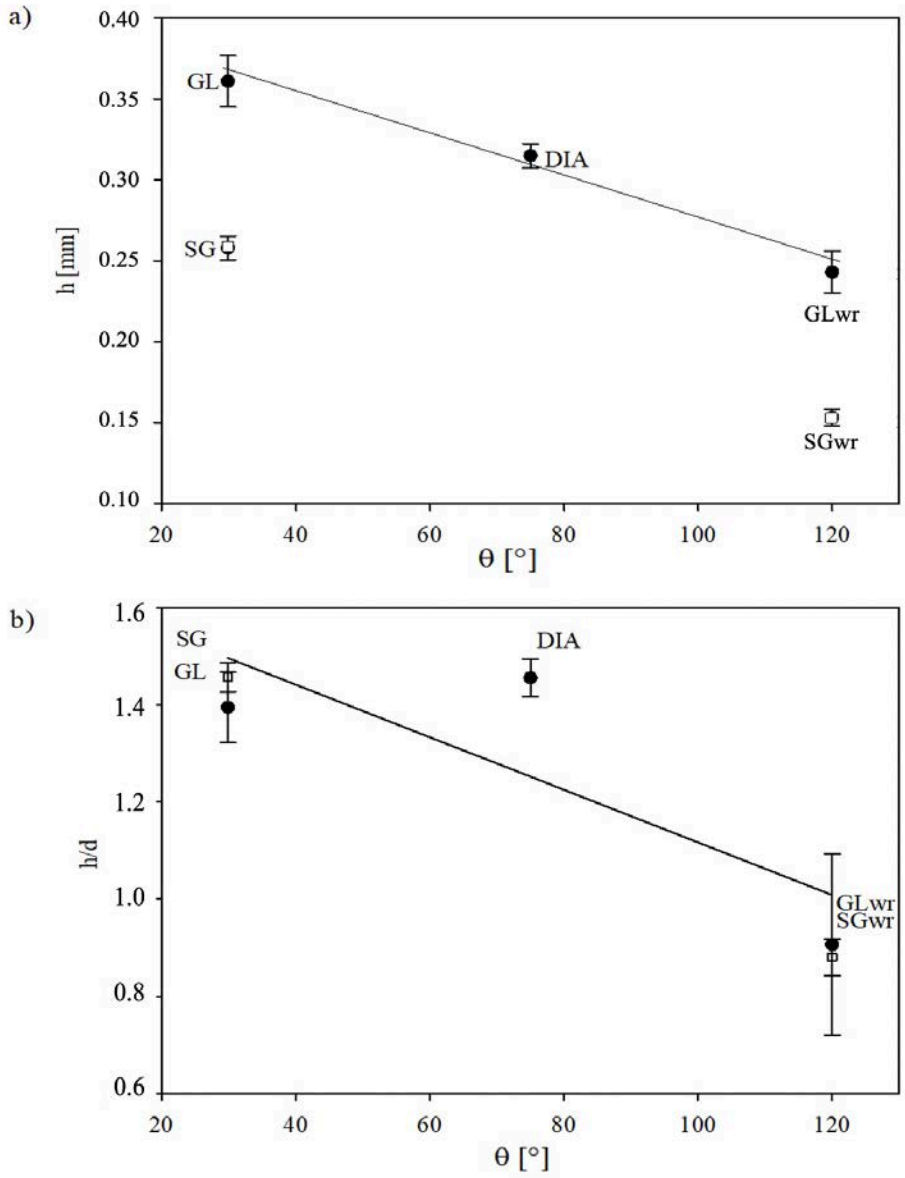

530

531 **Figure 4: a) Contact angle (CA) of bulk material *vs* height of water lamella and, b) CA of bulk**

532 **material *vs* lamella height normalized by particle diameter. Whiskers represent standard**

533 **errors. N=5 for each sample type.**

534

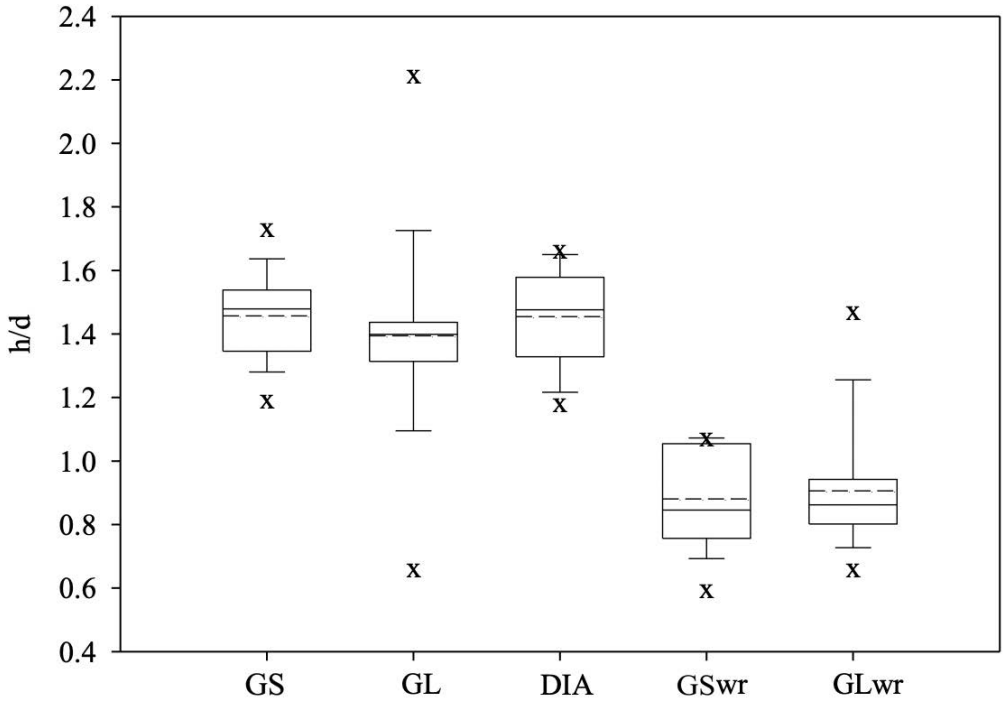

535

536 **Figure 5: Distribution width of the dimensionless ratio *h/d* for each sample. Boxes represent**
537 **50% of the distributions bearing solid and dashed lines indicating their median and mean**
538 **values (respectively) and with upper and lower whiskers representing the 90th and 10th**
539 **percentiles respectively. The x represents maximum and minimum values.**

540

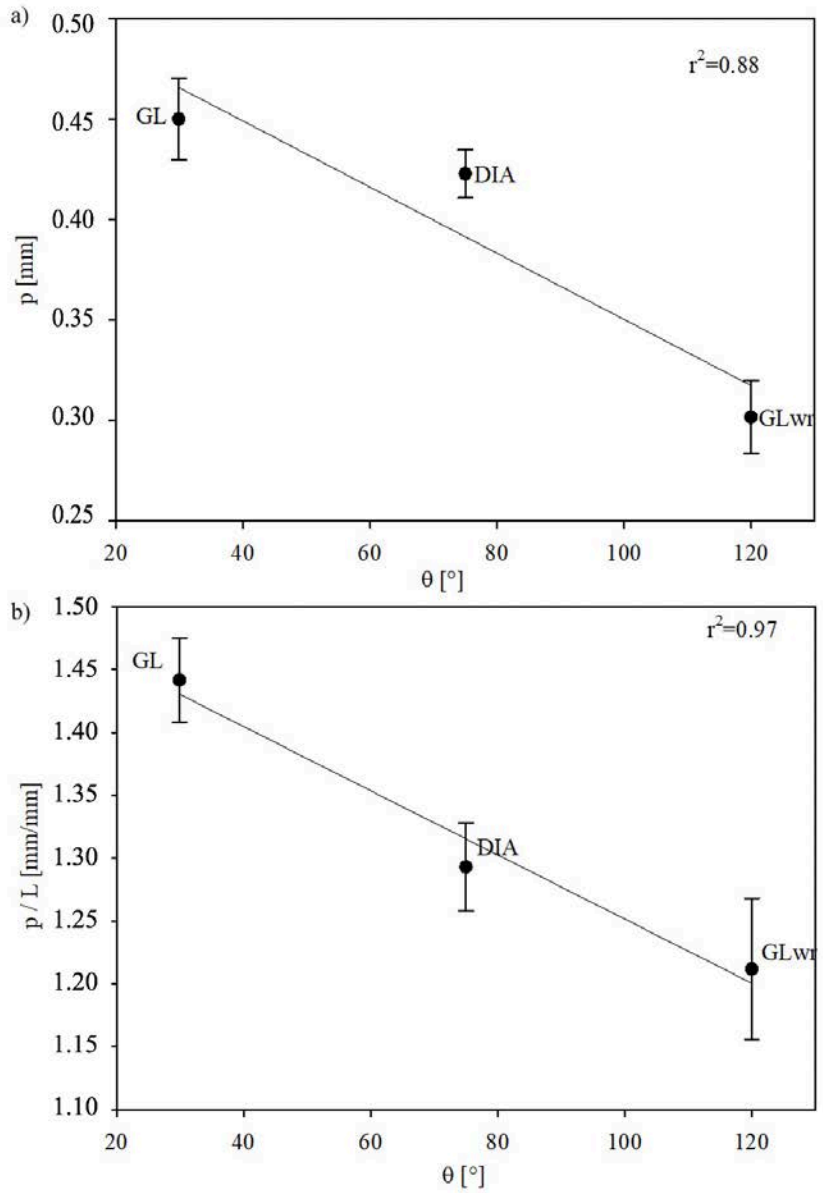

541

542 **Figure 6: a) position of sample (*ps*) relative to liquid surface *vs* contact angle *θ* on a smooth**

543 **surface and b) p normalized by wetted length (*L*) *vs θ*. Error bars equal standard error.**

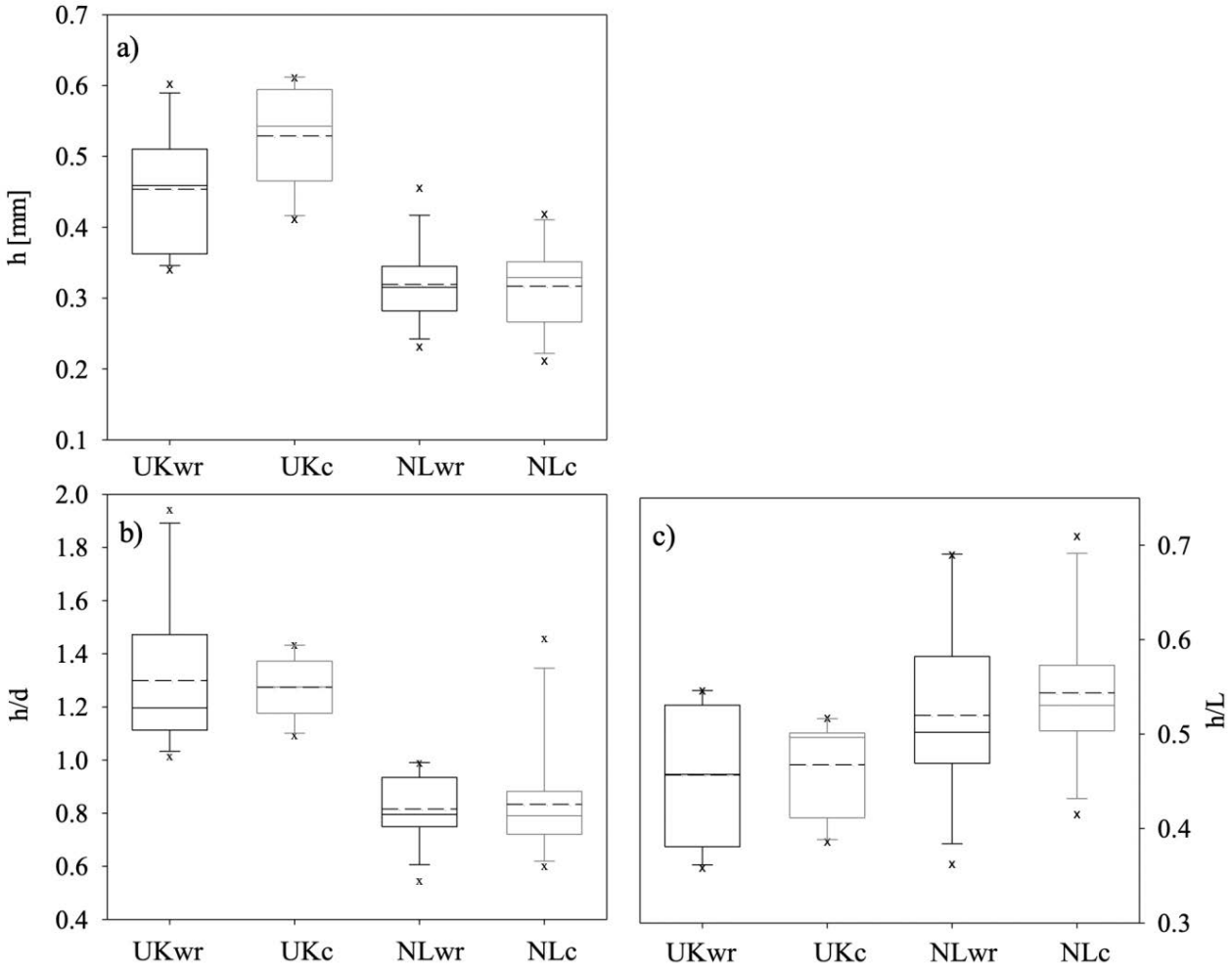

544

545 **Figure 7: Box plots of the distribution of (a) h, (b) h/d and (c) h/L of various soil samples. The**

546 **dashed line represents the arithmetic mean, the solid horizontal line the median and x outliers.**

547

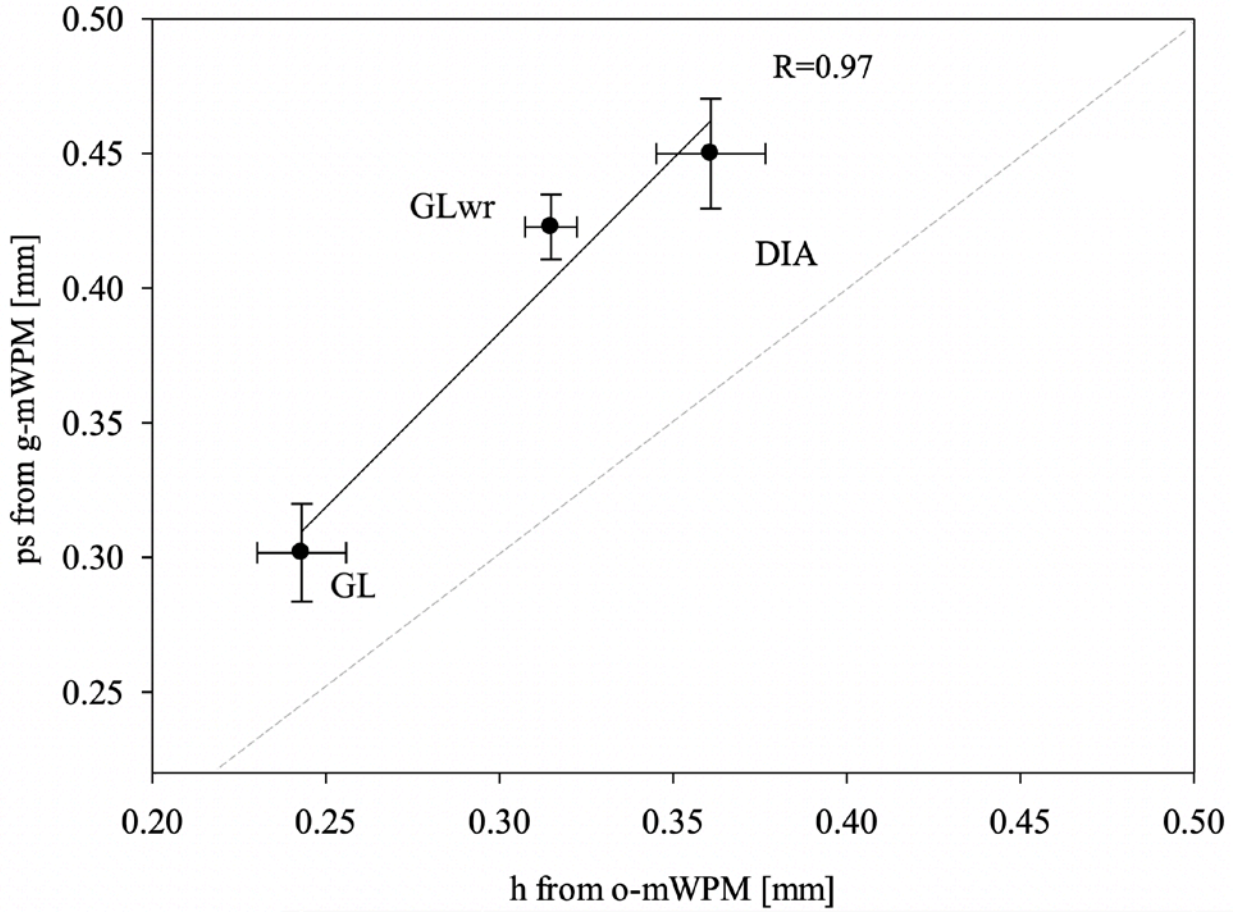

Figure 8: Mean lamella heights determined by tensiometer (g-mWPM) *vs* goniometer (o-mWPM), their linear correlation and 1:1 line (dashed).